JOURNAL OF Applied Polymer SCIENCE

Influence of Laminate Thickness Reduction on the Deformation Mechanism of Coextruded Multilayered PC/PMMA Films

Stefanie Scholtyssek,[1] Volker Seydewitz,[1] Rameshwar Adhikari,[2] Frank Pfeifer,[3] Goerg Hannes Michler,[1] Heinz Wilhelm Siesler[3]

[1]Institute of Physics, Martin-Luther-University Halle-Wittenberg, D-06099 Halle (Saale), Germany
[2]Central Department of Chemistry, Tribhuvan University, Kathmandu, Nepal
[3]Department of Physical Chemistry, University of Duisburg-Essen, D-45117 Essen, Germany
Correspondence to: S. Scholtyssek (E-mail: stefanie.scholtyssek@physik.uni-halle.de)

ABSTRACT: The influence of the morphology of multilayered composites of poly(methyl-methacrylate) (PMMA) and polycarbonate (PC) fabricated by layer multiplying coextrusion technique on their mechanical and especially their micromechanical deformation behavior was investigated. Electron microscopic studies revealed that the PC/PMMA multilayered composites have a well-oriented, uniform, and continuous layered architecture. With decreasing layer thickness of each polymer in the composite, the elongation at break of the films was found to increase significantly which was correlated with a transition from a two-component behavior (for single-layer thickness of $\geq$8 μm) to an one-component behavior (for single-layer thickness of $\leq$250 nm). Rheo-optical measurements using FTIR spectroscopy revealed that the molecular orientation during stretching of the PMMA phase remains unchanged for all the investigated films, whereas the PC orientation function decreases with decreasing layer thickness. © 2012 Wiley Periodicals, Inc. J. Appl. Polym. Sci. 000: 000–000, 2012

KEYWORDS: nanolayers; electron microscopy; FTIR; mechanical properties

Received 13 October 2011; accepted 7 May 2012; published online
DOI: 10.1002/app.38026

INTRODUCTION

Microstructured and nanostructured materials including those having layered architectures with specific mechanical or functional properties are in the focus of present research in the field of materials science and engineering. The aim is to produce materials having the good properties of the combined single materials or in ideal conditions even superior properties. One technique to produce ultrathin polymer layers is the multilayer coextrusion fabricating films with tens to thousands of alternating polymer layers.[1] The design and subsequent investigation of ultrathin and sometimes highly constrained polymer layers encompasses the understanding of the size-scale dependent properties as bulk polymers become thinner and more two-dimensional.

An overview on the investigations of different multilayered polymers is given in Ref. 2. Most of the examined systems refer to combinations of two amorphous polymers. The combinations of poly(styrene-acrylonitrile) (SAN) and polycarbonate (PC),[3–5] and polystyrene (PS) and poly(methylmethacrylate) (PMMA)[6] are well known examples. Morphology and micromechanical properties are examined by optical microscopy (OM), scanning electron microscopy (SEM) and sometimes by atomic force microscopy (AFM). Moreover, there are only a few studies on combinations with at least one crystalline polymer.[7–10] Also the combination of two amorphous polymers such as PC and PMMA, which will be the object of this article, has been already addressed to some extent in the literature.[11,12] Reference 11 describes the irreversible deformation and yielding in microlayered PC/PMMA films with varying composition and number of layers. Increasing the number of layers—that means decreasing the single layer thickness—leads to an increase of elongation at break.

The present article focuses on the investigation of the influence of single laminate thickness of the PC/PMMA composites on micromechanical mechanisms of deformation. In contrast to the earlier works on similar systems, the special emphasis will be laid on the nanolayered polymers. The goal of this work is twofold: first the investigation of the structure development during multilayer coextrusion and second the investigation of the deformation mechanisms. Therefore, direct imaging techniques (such as SEM, transmission electron microscopy (TEM), and AFM) and tensile testing are used. Additional information on the micromechanical behavior will be extracted from rheo-optical Fourier-transform infrared spectroscopy measurements as described in Ref. 13.

Table I. Characteristics of the Investigated Multilayered PC/PMMA Films Including the Calculated Thicknesses of the Single PC and PMMA Layers and the Measured Thicknesses of Single PC Layers in the Multilayered PC/PMMA (50/50) Films

Number of layers	Film thickness (μm)	Calculated PC and PMMA single layer thickness	Measured PC single layer thickness	
			Mean value	Standard deviation
8 layers.	250	31 μm	30.4 μm	1.9 μm
8 layers	125	16 μm	21.4 μm	1.6 μm
32 layers	250	8 μm	10.6 μm	1.4 μm
32 layers	125	4 μm	4.9 μm	0.6 μm
1024 layers	250	250 nm	265 nm	49 nm
1024 layers	125	125 nm	149 nm	44 nm
4096 layers	125	30 nm	27 nm	6 nm
4096 layers	50	12 nm	9 nm	3 nm

EXPERIMENTAL

Materials and Sample Preparation

The materials used in this work are multlilayered composite films comprising alternating layers of PC (Calibre 300-15 (DOW), molecular weight 27,000 g/mol), and PMMA (V826-100 (Ato-Haas), molecular weight 120,000 g/mol). To produce these composites, the well established multilayer coextrusion procedure[1] was used at Case Western Reserve University (CWRU), Cleveland, Ohio, USA. The single-layer thicknesses of the described samples calculated from the processing parameters vary from 31 μm down to only 12 nm. The composition by volume of each film is 50/50. An overview of the samples investigated in this work is given in Table I.

Microscopic Techniques

Morphology of the samples with the single layers having thickness of several microns was investigated by SEM (JEOL 6300, JEOL, Tokyo, Japan) operated at an accelerating voltage of 15 kV. Prior to the SEM examination, the cross-section of each sample was treated with a permanganic etchant (procedure according to Olley et al. and Olley and Bassett[14,15]). For the study of the morphology of the samples with the thickness of the single layers in the range of several nanometer, a TEM (LEO 912, Zeiss, Oberkochen, Germany) operated at an accelerating voltage of 120 kV was employed. For this purpose, the samples with properly prepared cross-sections were stained with ruthenium tetraoxide (RuO_4) vapor for several hours at 60°C. Then ultra-thin sections (80 nm thick) were prepared by an ultramicrotome (Ultracut E, Leica, Vienna, Austria) equipped with a diamond knife (Diatome, Biel, Switzerland) at room temperature.

For the study of deformation behavior of the samples, semithin sections (500 nm thick) were microtomed at room temperature using the diamond knife parallel to the extrusion direction as described in Figure 1. Following the deformation of each section in a special tensile stretching device, the sections were fixed in the strained state, transferred to the TEM specimen holder and directly studied in the TEM (JEM 4000FX, JEOL, Tokyo, Japan) operated at an accelerating voltage of 400 kV. For studying the deformation behavior, the samples were not stained during the complete preparation. Those studies were carried out at the Max Planck Institute for Microstructure Physics in Halle (Saale), Germany.

To compare the deformation behavior of the semithin sections described above with that of the bulk samples, an AFM (Digital Instruments Multimode Atomic Force Microscope equipped with NanoScope IIIa controler, Santa Barbara, California, USA) was used. The freshly ultramicrotomed surface of the tensile bar was directly scanned by the AFM in tapping mode using microfabricated silicon cantilevers of the type SuperSharpSilicon and High Aspects Ratio Probes (SSS-NCH50, Nanoworld, Neuchatel, Switzerland) with a tip radius of about 2 nm, a thickness of 4 μm, a length of 125 μm, and a width of 30 μm resulting in a resonance frequency of about 320 kHz and a force constant of about 42 N/m. Tapping mode investigations were carried out with a chosen free amplitude of about 77 nm and a reduced amplitude of about 62 nm (set point ratio = 0,8) corresponding to the selected set point.

Mechanical Testing

Tensile tests were performed according to the norms of DIN EN ISO 527 using miniaturized tensile test specimens (starting gauge length 50 mm). The specimens were punched out of the extruded films with their long axis along the extrusion direction. For the tests, a universal tensile machine (Zwick 1425, Ulm, Germany) was operated at room temperature at a crosshead speed of 50 mm/min (strain rate 100% per minute) measuring the traversal displacement of the cross-heads. To compare the tensile test results with the results from rheo-optical Fourier-transform infrared (FTIR) measurements, the tensile tests have been repeated with a strain of only 10% per minute.

The preparation of specimens from the films for examinations as well as for the tensile tests is schematically illustrated in Figure 1.

Rheo-Optical FTIR Investigations

Rheo-optical FTIR spectroscopy examinations were performed to examine the responds of the individual kinds of molecules in the layers toward tensile loading and to correlate the information with the results from tensile tests and TEM studies. During uniaxial elongation of small strips of each multilayered film FTIR spectra were recorded with the IR radiation polarized alternately parallel and perpendicular to the tensile direction.

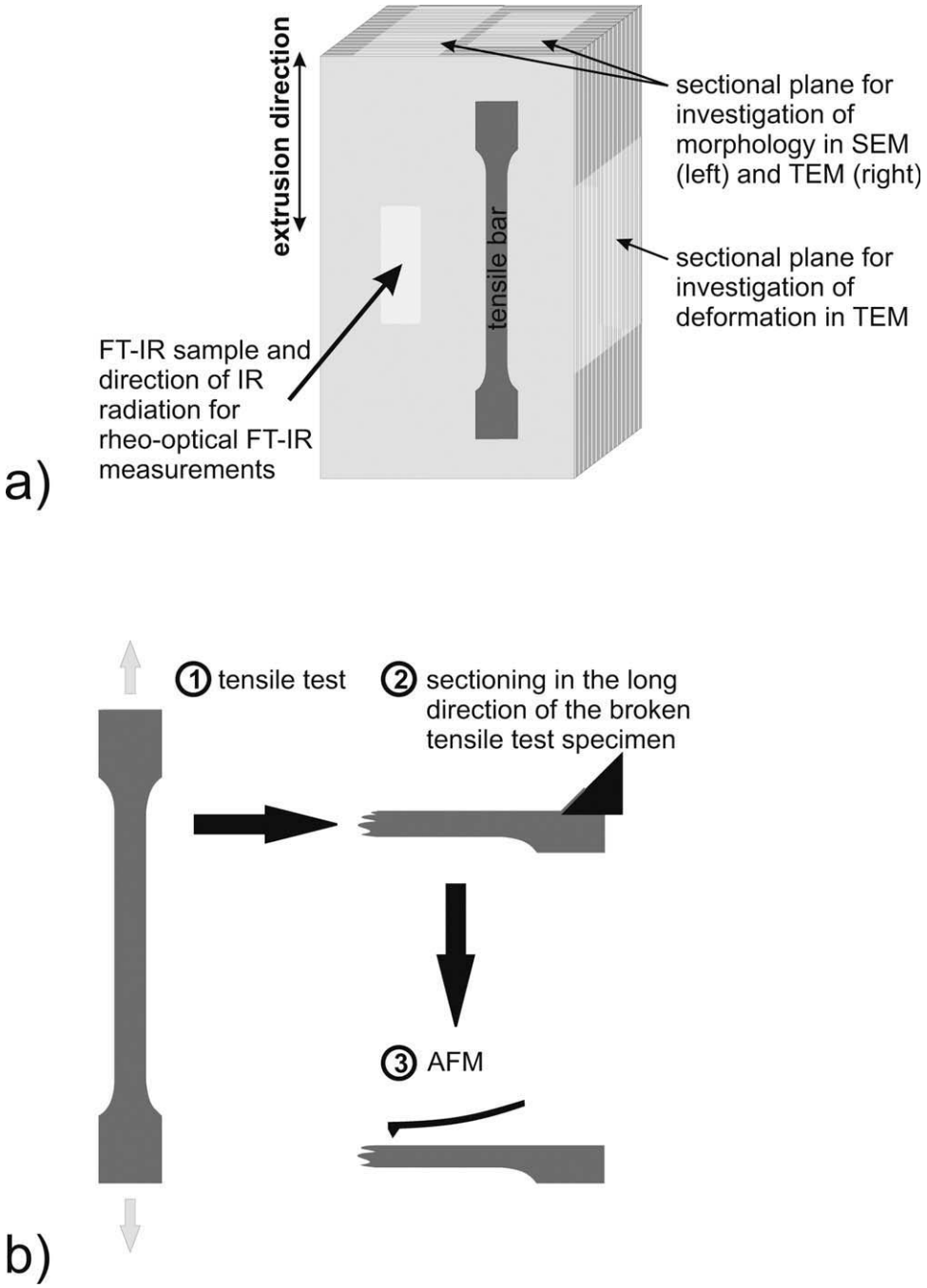

Figure 1. Scheme showing the preparation of (a) tensile test specimens for characterization of mechanical properties, TEM sections, and SEM cross-sections for investigation of morphology, TEM sections for investigation of deformation behavior and (b) cross-sections for investigation of deformation structures by the AFM.

The measurements were performed on a Bruker IFS 88 FTIR spectrometer (Bruker Optik GmbH, Ettlingen, Germany) equipped with an mercury cadmium telluride (MCT) detector. The spectral resolution was 4 cm^{-1} and 10 scans were accumulated in 3 s for one spectrum. In these experiments, a strain rate of only 10% per minute (10 times less than during tensile testing) was chosen in order to acquire enough FTIR spectra for the calculation of orientation function values during the mechanical treatment. The difference in strain rate between the mechanical testing and the rheo-optical investigations may lead to different forms of the stress–strain diagrams because of the known time dependence of material behavior. Experiments were performed up to an elongation of 50% strain.

RESULTS AND DISCUSSION

Characterization of Multilayer Film Morphology

Due to the presence of a wide range of calculated layer thicknesses two different electron microscopic techniques were used

for the investigation of multilayer film morphology. The first one was the SEM examination of the cross-sectioned films after permanganic etching. The results are presented in Figure 2. In the SEM images, the PC layers appear smooth whereas the PMMA layers are rough and uneven revealing the formation of voids. This difference is caused by the etching. While PC remained almost unaffected the PMMA was strongly attacked by the etchant leading to the formation of rougher and voided surfaces. The covering PMMA surfaces are abolished by the etchant. Therefore in Figure 2(a,c) only seven layers can be seen, even though the original film contains eight layers.

For the films with layers, only few nanometers thin ultra-thin sections were inspected by means of TEM. The results are illustrated in Figure 3 where PC (the stained phase) appears dark and PMMA (the unstained component) bright.

The micrographs of all the samples presented in Figures 2 and 3 nicely reveal the alternating layers of PC and PMMA. The layers are uniform and continuous. It is evident that the films containing thicker microlayers have no or only little defects.

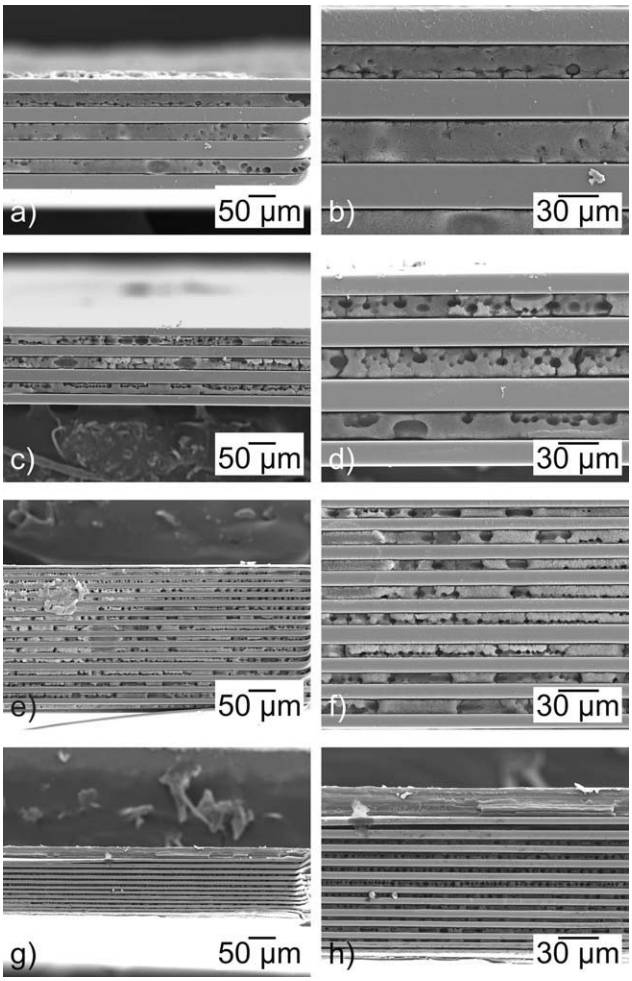

Figure 2. Lower (left) and higher (right) magnifications of SEM micrographs of the etched PC/PMMA multilayered films with variable calculated layer thickness of several μm, (a+b) layer thickness 31 μm, (c+d) layer thickness 16 μm, (e+f) layer thickness 8 μm, (g+h) layer thickness 4 μm.

The PC layer thicknesses measured on SEM and TEM micrographs, respectively, correspond very closely to the calculated values. The results are given in Table I. At first glance it can be observed that calculated and measured layer thicknesses are approximately the same indicating a successful multilayer coextrusion of the polymers into the layered architectures. The standard deviation of the measured layer thickness is very small for the films with layer thicknesses of several microns. It can be concluded that there is only a narrow distribution in layer thickness. Thus, it is possible to coextrude films with desired layer thicknesses.

When the calculated layer thickness is in the nanometer range, the standard deviation is an order of magnitude higher (see Table I). The distribution in layer thickness is much wider than in the earlier case. Additionally, there is probably a higher error in the measurement of the thinner layers.

In the present work, the layer-thickness measurements were focused on PC layers. In the SEM images, the PMMA layers cannot be estimated with precision as the PMMA phase was strongly etched. For the TEM images, the estimation of PMMA layer thickness was more difficult as the PMMA phase becomes unstable and expanded (leading to thicker layers) during the TEM examination. Thus, due to the electron irradiation induced artifacts, the PMMA layers appear wider than the actual thickness—imposing the difficulty in precise layer thickness estimation using TEM micrographs.

Characterization of Mechanical and Micromechanical Properties

In this section, the correlation between the observed morphology and the mechanical properties is discussed. Table II characterizes the mechanical properties of the composites depending on film thickness and number of layers. The corresponding stress–strain curves (one characteristic of at least 3 replicate measurements) of the samples, recorded with two different strain rates, are given in Figure 4. The values indexed in Table II are the mean values of at least three independent measurements in each case.

At constant number of layers but reduced film thickness—this means also a reduction in thickness of each layer—the Young's modulus (E) is constant. Overall, the value of E lies between 3200 MPa and 3300 MPa. The tensile strength (σ_M) of the composites fluctuates slightly from 67 MPa to 77 MPa. Both, Young's modulus and tensile strength values, do not seem to have any particular trend. In contrast, the elongation at break (ε_B) is considerably affected by the layer thickness. When the layer thickness is in the range of several microns the increase in ε_B with decreasing layer thickness is only a trend but it becomes significant when the layers are in the range of several nanometers (see Table II). It can be shown that the brittle multilayered PC/PMMA system gets more ductile if the layers are sufficiently thin. With the 12 nm thin layers a mean value of the elongation at break of about 14.7% (individual values up to 19%) is possible for strain rates of 100%. Strain rates of only 10% allow a mean value of 70% and individual values up to

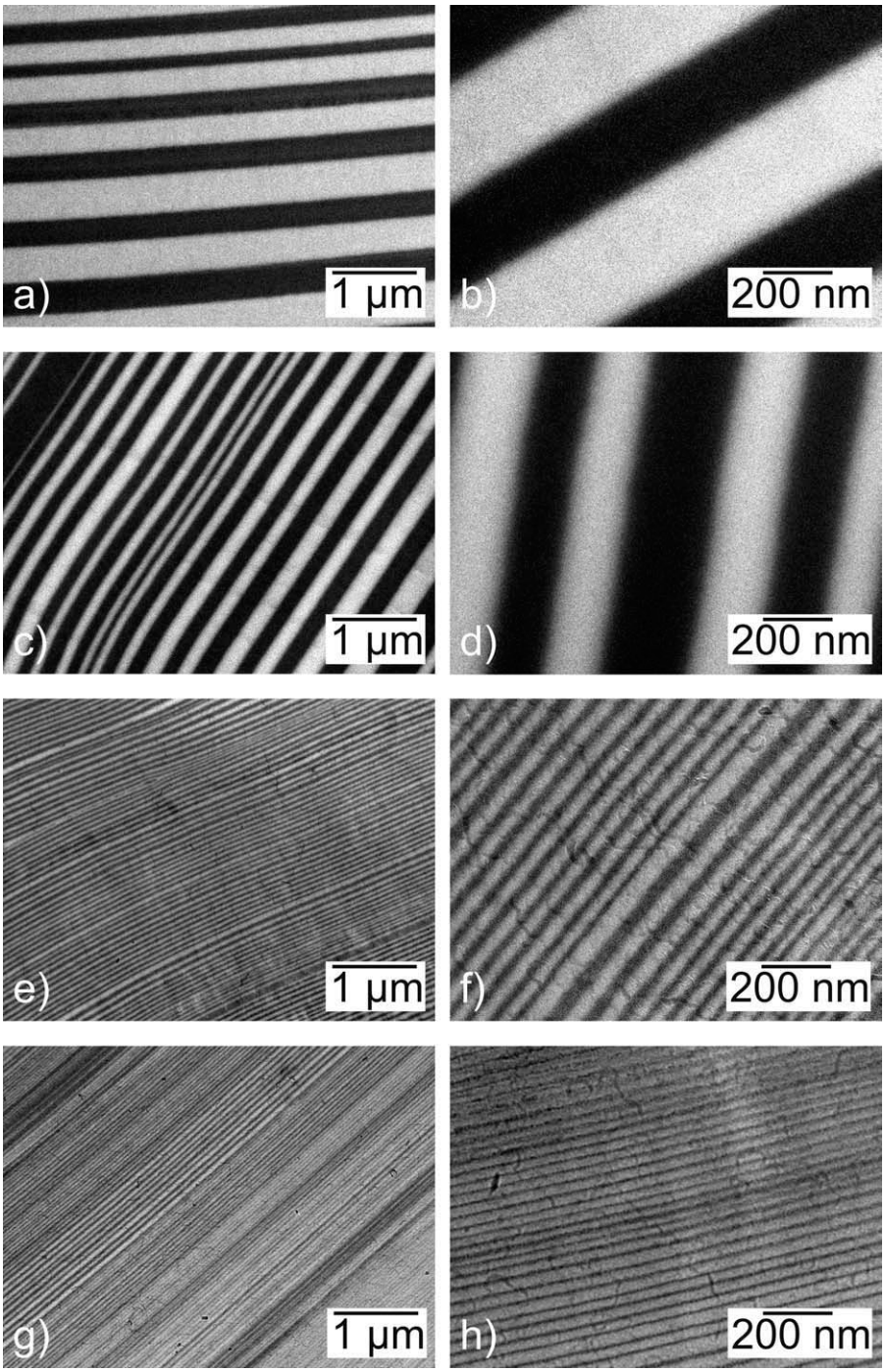

Figure 3. Lower (left) and higher (right) magnifications of TEM micrographs of the stained PC/PMMA multilayered films having variable calculated layer thickness, (a+b) layer thickness 250 nm, (c+d) layer thickness 125 nm, (e+f) layer thickness 30 nm, (g+h) layer thickness 12 nm.

80%. Overall, one should keep in mind that the elongation at break of bulk PMMA is about 2–10%[16] which is clearly less than that what can be reached in the multilayered composites. The pronounced improvement in ε_B begins when the layer thicknesses are in the nanometer range (practically when $d \leq$ 250 nm, see also Figure 5). The elongation at break of bulk PC is about 100–130%.[16] It is much higher than the value reached with the multilayered film having a single layer thickness of about 12 nm (strain rate 100%). Similar results could be found for the multilayered system polypropylene/PS.[17] The elongation at break of the multilayered films increased by decreasing the layer thickness and elongation at break was much higher than that of brittle bulk PS. An approach of the mean values of the multilayered films to the value of the ductile bulk polypropylene just appeared when the PP content in the film was considerably higher than 50%.

Table II. Mechanical Properties of PC/PMMA (50/50) Composites Determined by Tensile Testing at 23°C

Number of layers	Film thickness (μm)	PC and PMMA single layer thickness (calculated)	Young's modulus (MPa)	Tensile strength (MPa)	Elongation at break (%)
Strain rate 100%/min (cross-head speed 50 mm/min)					
8 layers	250	31 μm	3210 ± 108	67 ± 6.9	2.7 ± 1.0
8 layers	125	16 μm	3199 ± 110	71 ± 3.4	3.2 ± 0.5
32 layers	250	8 μm	3362 ± 178	78 ± 2.7	3.6 ± 0.8
32 layers	125	4 μm	3313 ± 94	73 ± 2.9	4.1 ± 0.9
1024 layers	250	250 nm	3131 ± 132	77 ± 1.8	6.3 ± 0.9
1024 layers	125	125 nm	3240 ± 208	77 ± 1.7	5.8 ± 1.4
4096 layers	125	30 nm	3342 ± 133	74 ± 3.0	9.3 ± 1.7
4096 layers	50	12 nm	3116 ± 46	69 ± 0.3	14.7 ± 7.2
Strain rate 10%/min (corresponding to rheo-optic FTIR)					
8 layers	250	31 μm	not measured	60 ± 1.0	19 ± 2.5
8 layers	125	16 μm	not measured	57 ± 1.0	16 ± 1.7
32 layers	250	8 μm	not measured	59 ± 2.6	30 ± 4.2
32 layers	125	4 μm	not measured	62 ± 2.8	47 ± 10.3
1024 layers	250	250 nm	not measured	60 ± 1.0	63 ± 10.1
1024 layers	125	125 nm	not measured	62 ± 0.7	56 ± 4.4
4096 layers	125	30 nm	not measured	62 ± 3.3	43 ± 9.3
4096 layers	50	12 nm	not measured	69 ± 11.1	70 ± 9.5

A possible explanation for the observed results is that the molecular mobility, which is eventually responsible for the elongation at break, is influenced by the layer thickness through confinement leading to an arrangement of molecules in much different manner than in bulk polymers. On the contrary, Young's modulus depends on the bond strength and orientation of molecules and less on molecular mobility. That is why there is no influence of layer thickness on the Young's modulus while the elongation at break is affected significantly.

The mechanical properties of the composites observed by tensile testing can be correlated with the micromechanical properties studied by TEM. The results are summarized in Figure 5. For 31-μm thick layers (250-μm thick film with eight layers) crazes in the PMMA layers and shear bands in the PC layers can be noticed [see Figure 5(a)]. Upon tensile loading, each layer responds as it was an individual bulk PMMA or PC sample (i.e., the behavior of the single component can be identified). When the layers become thinner [8 μm; Figure 5(b)] the crazes still can be seen in the PMMA layers and shear bands are visible in the PC layers. Nevertheless, a new phenomenon that can be observed herewith is that PMMA crazes pass slightly into the PC layers initiating the shear bands. It implies that the layers begin to influence each other upon tensile loading. That means the interphase between the layers is strong enough for stress transfer from one layer to the next. However, the material behavior is the same as before [compare Figure 5(a) and (c)]. In the macroscopic behavior, no difference could be observed between those two samples (see Figure 4 and Table II). By reducing the layer thickness down to 250 nm (250-μm thick film comprising 1024 layers) the micromechanical behavior changes dramatically [see Figure 5(e+f)]. Firstly, the crazes of classical nature vanish and, secondly, new kinds of shear bands going through the width of the specimen (i.e., through both PC and PMMA simultaneously) can be detected. Additionally, short crazes located inside the shear bands going through the PMMA layers can be found. Figure 5(e+f) illustrates that the single polymer layers do not respond as single components toward the tensile loading, instead the whole composite behaves as it is only one material. When the layers themselves are only 12 nm thin (50 μm thick film with 4096 layers) all deformation structures—crazes and shear bands—vanish [Figure 5(g+h)], but the sample itself is highly elongated as could be seen at the defects on the sample border [Figure 5(h)]. That means the whole sample deforms homogenously, which is entirely one-component behavior.

In summary, the behavior of the microlayered composites can be described as two-component behavior and that of the nanolayered composites as one-component behavior in agreement with results obtained on multilayered PET/PC systems.[18] The deformation mechanism of the one-component behavior changes as the layers become thinner.

A comparison of a deformed semithin section and a section in the long direction of a broken tensile test specimen of the PC/PMMA film with a single-layer thickness of 250 nm is shown in Figure 6. In the TEM image of the semithin section [Figure 6(a)], shear bands extending over the whole sample (that means over both, the PC and PMMA layers) and small crazes in the PMMA layers inside the shear bands can be found as described above. However, in the AFM image of the broken tensile test specimen [Figure 6(b)], no shear bands can be seen but it

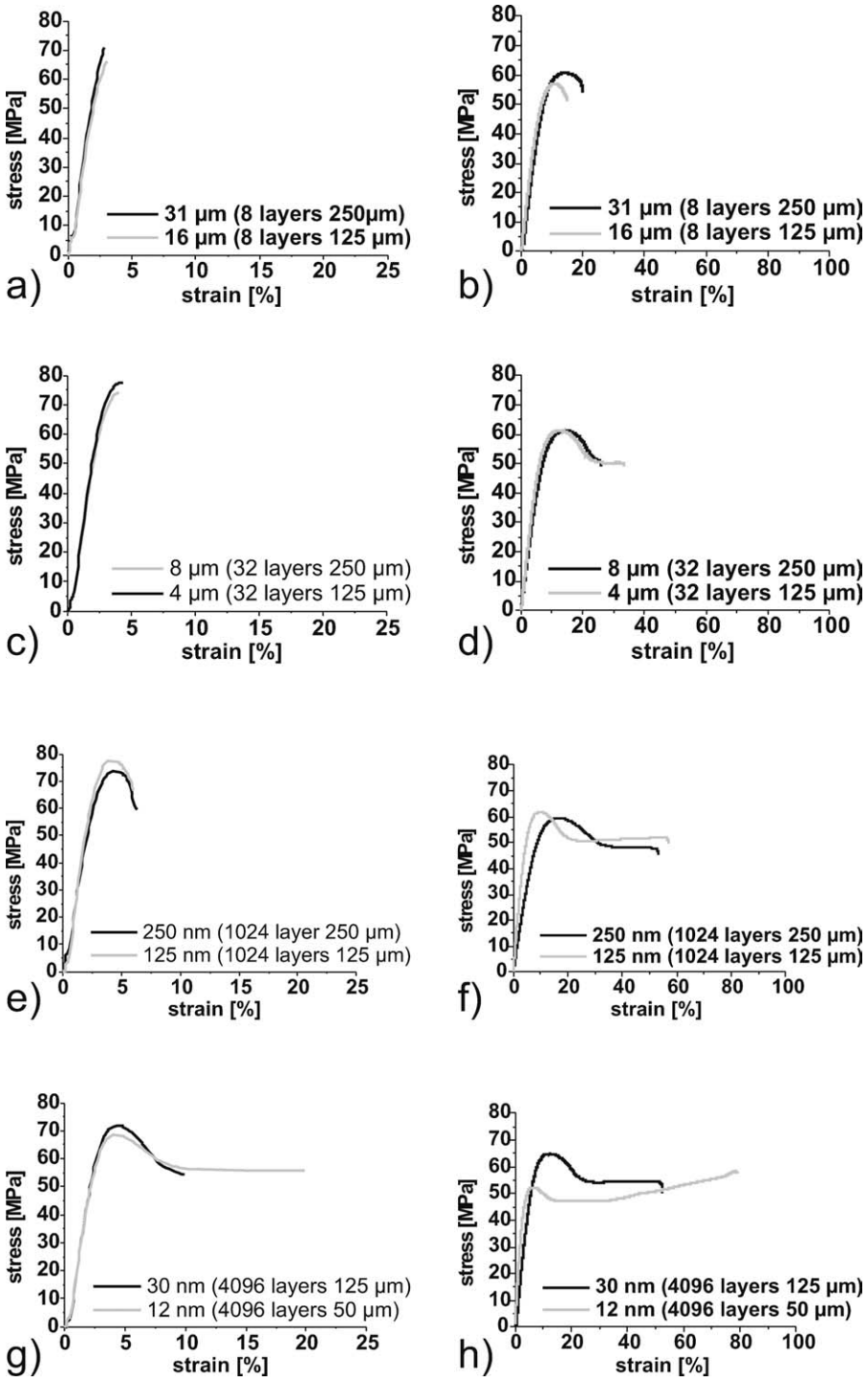

Figure 4. Stress–strain curves of the investigated samples recorded at 23°C with a strain rate of 100% per minute (left) and 10% per minute (right).

reveals short crazes in the PMMA layers. These are preferentially arranged in lines with an angle of approximately 45° to the tensile direction. The white lines showing the shear bands in the TEM image transferred to the AFM image lie directly on the lines of the PMMA crazes. That implies that the arrangement of the small crazes in the PMMA layers indicates the existence of shear bands in the tensile test specimen, too. A comparison of these two techniques leads to the conclusion that the deformation of the semithin sections is similar to the deformation of the films in the tensile test. So the TEM results on the semithin sections can be transferred to macroscopic samples.

Characterization of Molecular Deformation

For the characterization of the molecular alignment during deformation rheo-optical experiments as described above were performed for the films with single-layer thicknesses of 4 μm,

Applied Polymer SCIENCE

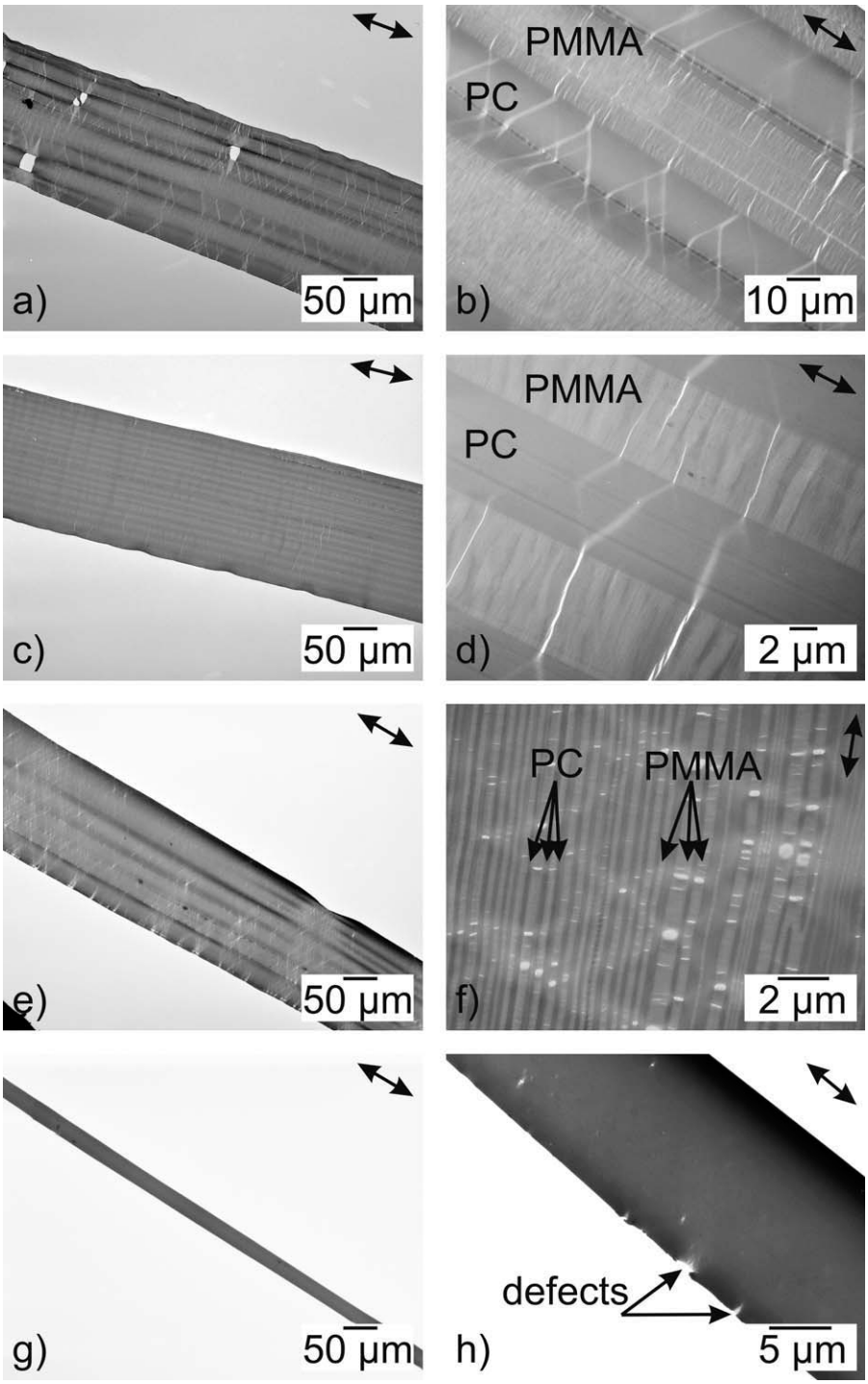

Figure 5. TEM micrographs of the deformed PC/PMMA multilayers, the arrows indicate the tensile direction (a+b) layer thickness 31 μm, (c+d) 8 μm, (e+f) 250 nm, (g+h) 12 nm, left: overview, right: higher magnification.

125 nm, and 12 nm. Since the FTIR spectra contain both the bands of PC and PMMA, it is difficult to find isolated bands for each polymer which provide information by the variation of dichroism during mechanical treatment. For the given multilayered system these are the combination band at 1900 cm^{-1} for PC and the first overtone of the ν(C=O) band at 3440 cm^{-1} for PMMA for the two films with the thicker layers. For the film with a single layer thickness of only 12 nm the left and right wings, respectively, of the ν(C=O) bands of PC (1775 cm^{-1}) and PMMA (1731 cm^{-1}) have been evaluated. For all the absorption bands, the transition moment direction was assumed to be perpendicular to the polymer chain direction. To demonstrate the polarization effects of the relevant absorption bands for 50% elongated PC/PMMA film with a layer thickness

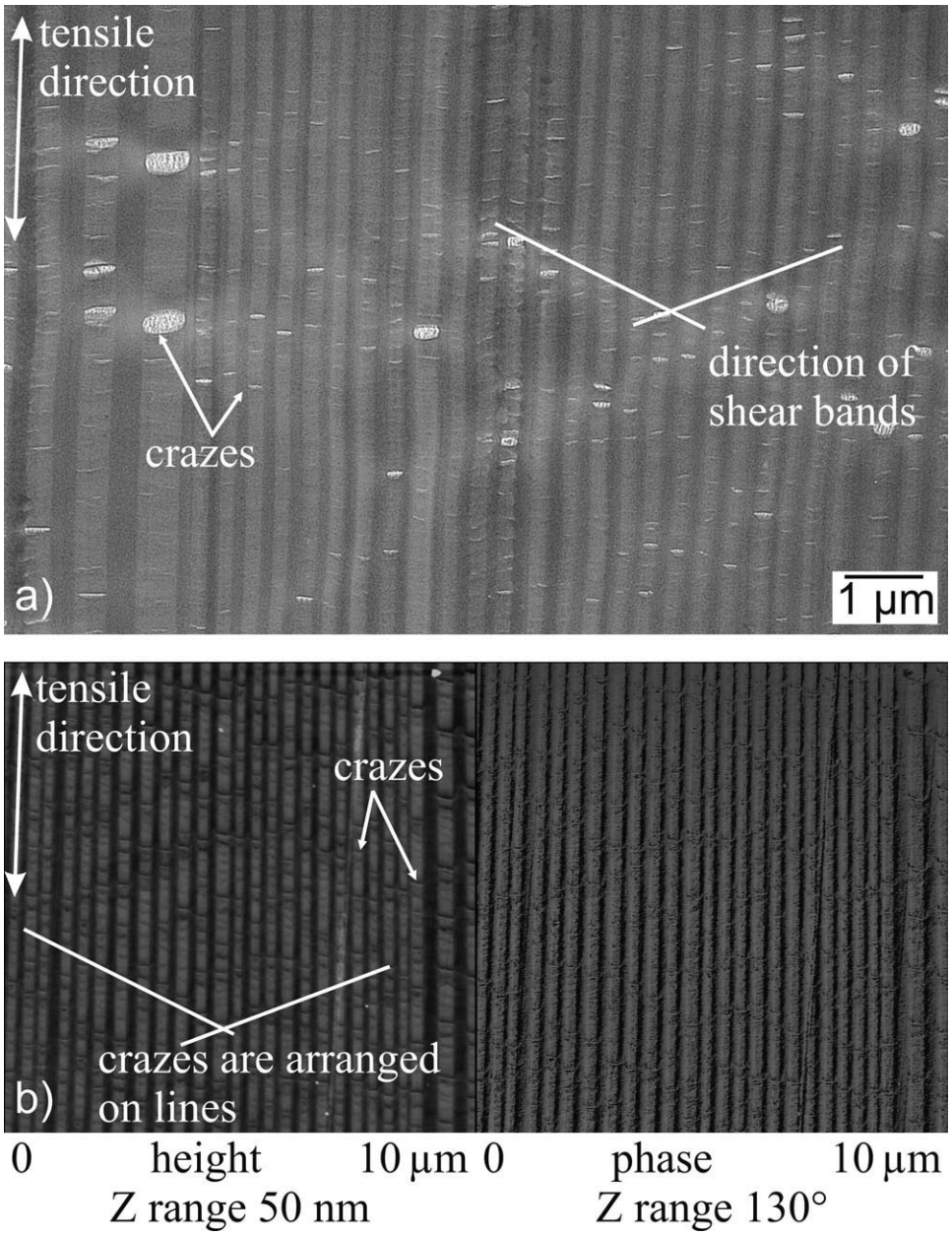

Figure 6. Comparison of (a) micromechanical behavior, TEM micrograph of a deformed semithin section and (b) mechanical behavior of miniaturized tensile test specimen, AFM image of a cross sectioned tensile test specimen broken during the tensile test, the sample for both (a) and (b) is PC/PMMA with a layer thickness of 250 nm.

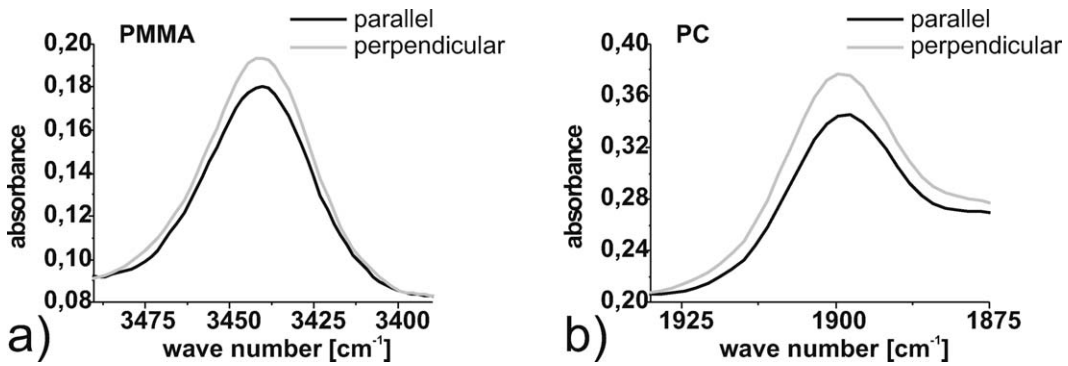

Figure 7. Polarization spectra of the PMMA and PC specific absorption bands for the 125 μm thick PC/PMMA film with a single layer thickness of 4 μm at 50% uniaxial elongation.

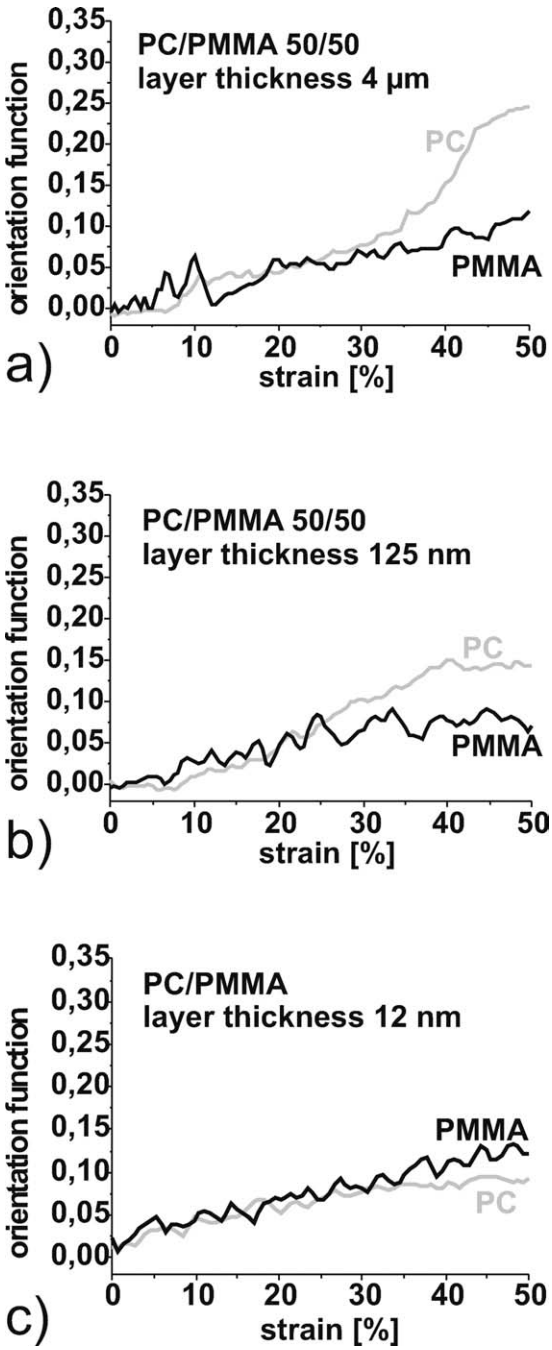

Figure 8. Comparison of the orientation functions of the PC/PMMA films having different layer thicknesses (a) 4 μm, (b) 125 μm, and (c) 12 nm.

of 4 μm, the two spectral regions are shown in Figure 7. Figure 8 presents the calculated orientation functions of different composites as a function of tensile strain. When the orientation function is 0, this means that the molecules are statistically arranged and have no preferential orientation. A value of 1 implies that all molecules are perfectly aligned parallel to the tensile direction.

What could be learned from the orientation functions is that the polymer chains of all the specimen orient into tensile direction during elongation. But the fact that the shapes of the orientation functions are different for the three samples shows, that their deformation behavior is different—as it is shown in Figure 6. Figure 8 shows that the orientation of the PC and PMMA molecules in the films with the thicker layers is different. The orientation of PMMA rises constantly from the beginning of experiment. Up to a strain of 7% the PC molecules of the thicker layers have no preferred orientation. Above the strain of 7% the orientation of PC increases in a steady state. At the end of the experiment at a strain of 50% the orientation of PC is higher than the orientation of PMMA. It can be seen that the degree of orientation of PC molecules decreases by decreasing the layer thickness, whereas the degree of PMMA orientation is approximately the same for all three films. For the film with the 12 nm thin layers the orientation functions of the PC and the PMMA molecules are about the same implying that the deformation behavior of the PC and PMMA chains is the same for this film. This observation is consistent with the microscopic results of this film which deforms homogenously. Liu et al.[19] found that the interphase between PC and PMMA layers is about 10 nm thick. That means that films with single layer thicknesses of 12 nm consist primarily of interphase material. As a result, both kinds of layers—PC and PMMA—exhibit the same behavior of molecular orientation during straining the composite comprising the 12 nm thin layers. The higher orientation of the PC molecules in the films with the layers thicker than 12 nm can be explained as follows: PC deforms with shear bands and PMMA with crazes. In the shear bands a large number of polymer chains align into the tensile direction while in the crazes, there are only a few fibrils with molecules aligned parallel to the tensile direction. The orientation of these few polymer chains is definitely higher than the orientation of the molecules in the shear bands. But the orientation functions presented here are calculated from infrared measurements of on an area of a few square millimeters. That means the orientation functions present integrated values of deformed areas (shear bands and crazes) and non-deformed areas. Therefore the orientation function of a material deforming with shear bands like PC must be higher than for a material deforming with crazes like PMMA.

The fact that the molecules keep orienting up to the end of the experiment implies that both PC and PMMA layers are still intact up to the end of the experiment as was shown in micromechanical deformation tests with TEM where the layers remained undelaminated even at large deformation (see Figures 6 and 8).

CONCLUSIONS

The morphology and the deformation behavior of the multilayered PC/PMMA films fabricated by layer multiplying coextrusion technique have been evaluated by means of electron microscopy and rheo-optical FTIR measurements. Uniaxial tensile testing was used to determine the macroscopic mechanical behavior of the composites. The findings of this work can be summarized as follows:

- The multilayered PC/PMMA composites have well oriented, uniform, and continuous layered architecture.

- With decreasing layer thickness of each polymer in the composite, the elongation at break of the films is found to increase significantly. This result can be correlated with a transition from a two-component behavior (for single-layer thickness of $\geq$8 μm) to the one-component behavior (for single-layer thickness of $\leq$250 nm). When the layer thickness decreases to only 12 nm there is a second transition in deformation mechanism. The film deforms homogeneously which can be explained by the fact that this film consists primarily of interphase material.
- Rheo-optical FTIR measurements show that PC and PMMA polymer chains orient into the stretching direction during tensile deformation. At the end of experiments at a strain of 50% the orientation of PC is higher than that of PMMA in the films having a layer thickness of 4 μm and 125 nm. For the film consisting of only interphase material the orientation functions of both the components are about the same, which is confirmed by the results above.

ACKNOWLEDGMENTS

The authors extend their sincerest thanks to Prof. E. Baer and Prof. A. Hiltner (Case Western Reserve University, Cleveland, Ohio, USA) for providing the multilayered films. Furthermore, the discussions which helped to continue the work on the materials are highly appreciated. The authors also acknowledge the German Research Foundation (DFG) and Max-Buchner-Forschungsstiftung for generously providing the financial support and Research Scholarship, respectively, to S. Scholtyssek. R. Adhikari acknowledges support of the Alexander von Humboldt (AvH) Foundation for providing fellowships.

REFERENCES

1. Mueller, C.; Kerns, J.; Ebeling, T.; Nazarenko, S.; Hiltner, A.; Baer, E. *Polym. Process Eng.* **1997,** *97*, 137.
2. Bernal-Lara, T. E.; Ranade, A.; Hiltner, A.; Baer, E. In Mechanical Properties of Polymers Based on Nanostructure and Morphology; Michler, G. H.; Baltá-Calleja, F. J., Eds.; Taylor and Francis Group: Boca Raton, London, New York, Singapore, **2005;** Chapter 15.
3. Ma, M.; Vijayan, K.; Im, J.; Hiltner, A.; Baer, E. J. *Mater. Sci.* **1990,** *25*, 2039.
4. Haderski, D.; Sung, K.; Im, J.; Hiltner, A.; Baer, E. J. *Appl. Polym. Sci.* **1994,** *52*, 121.
5. Sung, K.; Haderski, D.; Hiltner, A.; Baer, E. J. *Appl. Polym. Sci.* **1994,** *52*, 147.
6. Ivan'kova, E. M.; Krumova, M.; Michler, G. H.; Koets, P. P. *Colloid Polym. Sci.* **2004,** *282*, 203.
7. Jin, Y.; Rogunova, M.; Hiltner, A.; Baer, E.; Nowacki, R.; Galeski, A.; Piorkowska, E. J. *Polym. Sci. Part B: Polym. Phys.* **2004,** *42*, 3380.
8. Bernal-Lara, T. E.; Masirek, R.; Hiltner, A.; Baer, E.; Piorkowska, E.; Galeski, A. J. *Appl. Polym. Sci.* **2006,** *99*, 597.
9. Pan, S. J.; Im, J.; Hill, M. J.; Keller, A.; Hiltner, A.; Baer, E. J. *Polym. Sci. Part B: Polym. Phys.* **1990,** *28*, 1105.
10. Jin, Y.; Hiltner, A.; Baer, E.; Piorkowska, E.; Galeski, A. J. *Polym. Sci. Part B: Polym. Phys.* **2006,** *44*, 1795.
11. Kerns, J.; Hsieh, A.; Hiltner, A.; Baer, E. J. *Appl. Polym. Sci.* **2000,** *77*, 1545.
12. Kerns, J.; Hsieh, A.; Hiltner, A.; Baer, E. *Macromol. Symp.* **1999,** *147*, 15.
13. Hoffmann, U.; Pfeifer, F.; Okretic, S.; Völkl, N.; Zahedi, M.; Siesler, H. W. *Appl. Spectrosc.* **1993,** *47*, 1531.
14. Olley, R. H.; Hodge, A. M.; Bassett, D. C. *J. Polym. Sci. Part B: Polym. Phys.* **1979,** *17*, 627.
15. Olley, R. H.; Bassett, D. C. *Polymer* **1982,** *23*, 1707.
16. Oberbach, K. Kunststoff taschenbuch; Ausgabe, Carl Hanser Verlag: München Wien, **2001;** Vol. *28*.
17. Scholtyssek, S.; Pfeifer, F.; Seydewitz, V.; Adhikari, R.; Siesler, H. W.; Michler, G. H. *J. Appl. Polym. Sci.* **2012**; to appear.
18. Adhikari, R.; Seydewitz, V.; Löschner, K.; Michler, G. H.; Hiltner, A.; Baer, E. *Macromol. Symp.* **2010,** *290*, 156.
19. Liu, R. Y. F.; Jin, Y.; Hiltner, A.; Baer, E. *Macromol. Rapid Commun.* **2003,** *24*, 943.